UNCONVENTIONAL RESOURCES TECHNOLOGY CONFERENCE

URTeC: 4245581

Blind Testing Simulator Predictions of Refracturing Performance in the Bakken and the Permian Basin

Sama Morsy*[1], Chris Abbott[2], Mouin Almasoodi[3], Amanda Baldwin[3], Mohsen Babazadeh[4], Craig Cipolla[5], Kate Elliott[2], Agustin Garbino[1], John Lassek[5], Mike McKimmy[5], Chris Ponners[1], Mojtaba Shahri[6], Jose Zaghloul[2], and Mark McClure[1]

[1]ResFrac Corporation, [2]Continental Resources, [3]Devon Energy, [4]ConocoPhillips Company, [5]Hess Corporation, [6]APA Corporation

This paper was prepared for presentation at the Unconventional Resources Technology Conference held in Houston, Texas, USA, 9-11 June 2025.

Abstract

We performed numerical modeling of four refrac datasets – three from the Bakken and one from the Midland Basin. For each, history matching was performed to production data and diagnostic measurements from prior to the refrac. Then, the model was used to 'blind predict' the performance of the refracs. In the final step, the model prediction was compared with the actual production, and if needed, the inputs were updated to match the observed data. The simulations were performed with a fully integrated hydraulic fracturing and reservoir simulator. In a single simulation, the model incorporates the initial fracturing treatment(s), production, the refrac, and subsequent production. The integrated approach is advantageous for refrac because: (a) fluid crossflows into the original fracs during the refrac, resulting in multiphase oil/water/gas flow occurring simultaneously with fracture reopening, propagation, and proppant placement in the original fractures, and (b) the initial conditions of the refrac depend on the prior fracturing and production. After comparison with the field data, the blind refrac predictions were found to have good accuracy. On average, the refracs achieved a 26% uplift in the wells' cumulative production after one year. The smallest increase was 10%, and the largest increase was 57%. The average prediction mismatch in one-year cumulative production uplift was 3.7%. After unblinding, model recalibration was performed by modifying a parameter that controls the strength of crossflow outside casing.

1. Introduction

Refracturing provides a relatively small, but meaningful, contribution to production in unconventional resources (Lindsay et al., 2016; Morales et al., 2016; Brady et al., 2017; Dalkhaa et al., 2022; Bryan et al., 2023; Velasquez et al., 2023; Cui et al., 2023; Brinkley et al., 2023; Barba et al., 2024). Most commonly, refracturing is performed by cementing a new liner inside the original casing and performing multistage plug and perf completion. Less commonly, refracs are bullheaded by pumping directly from the surface

without utilizing any zonal isolation. Hybrid options are also available (Eichinger et al., 2023). Refracs may also be used as 'protection' fracs to reduce the impact of negative parent/child interactions from infill wells (Miller et al., 2016; Rezaei et al., 2017).

Refracture design poses a variety of practical engineering questions: (a) Is it best to refrac all wells or only some wells? (b) Should refracs be used as 'protection fracs' adjacent to new child wells? (c) Which wells are the best candidates for refracturing? (d) For a candidate well or pad, what is the optimal frac design and stage configuration? (e) Can we reliably predict the outcome of refracturing treatments?

In this study, we applied a combined hydraulic fracturing and reservoir simulator to four pad-scale refracturing datasets – BK1, BK2, BK3 (from the Bakken), and MB1 (from the Midland Basin). For each, we constructed a numerical model to match the pre-refrac data. Then, we performed a 'blind' prediction of post-refrac production and compare with actual results.

The goals of the study were to: (a) assess our ability to make blind predictions, and (b) identify if any changes or improvements to the default model inputs may be justified. A similar study was presented by Fowler et al. (2023) using a dataset from the Eagle Ford, showing good correspondence between the actual and 'blinded' predicted production.

2. Methods

Simulations were performed with a combined hydraulic fracturing and reservoir simulator (McClure et al., 2024). In each timestep, the simulator solves for: (a) mass balance on fluid components (oil, water, and gas when using the black oil fluid model), frac fluid additives, and proppants, (b) momentum balance in the wellbore, (c) fracture-to-fracture stress shadow calculations, and (d) porothermoelastic stress changes from depletion. The simulator accounts for perforation pressure drop and 'crossflow outside the casing' due to flow through the annular region and/or from a longitudinal fracture. Fractures are meshed as true 'cracks' and fracture mechanics calculations are used to predict fracture propagation and height growth (Dontsov, 2022). Because the simulator couples fracturing and multiphase flow, it can be used to simulate the full life-cycle of the pad in a single continuous simulation – generations of wells that are fractured, produced, and refractured.

When performing model calibration, we start by building a list of 'key observations' that characterize the dataset. This may include diagnostics such as Volume to First Response (VFR) and fiber, production data, and/or treatment pressure data. Model input parameters that may be varied include permeability, relative permeability, the stress profile, and fracture toughness.

When simulating wells with cemented casing, the model assumes that one fracture may initiate at every perforation cluster or port. In-situ observations suggest that fracture propagation may be multistranded. To address this phenomenon, adjustments may be made to fracture toughness, leakoff, viscous pressure drop, and/or production (McClure et al., 2020; Section 19.11 from McClure et al., 2024).

When simulating wells with uncemented casing, it is not obvious how many fractures should initiate and propagate from each stage. There is no 'perforation pressure drop' to force fractures to form and propagate at relatively tight spacing. Instead, stress shadowing tends to permit only a small number of fractures to form and propagate. Uncemented liners are not commonly used in modern wells; however, when modeling refracs or parent/child scenarios, we often need to history match from wells that used older-style designs. Many of these wells used uncemented liners, especially in the Bakken. Typically, we have found that it is sufficient to assume one, two, or three fractures per stage when an uncemented liner was used. In this study, the 'number of fractures per stage' was used as a history matching parameter. In particular, the BK2 dataset had already been subject to extensive calibration to data from the operator (Singh et al., 2025). Therefore, the number of fractures per uncemented stage was the *only* parameter that was varied as part of the history matching process for that dataset.

To reduce computational burden, the simulations usually include only one stage per well. Then, the results are 'scaled-up' to the full-lateral. This approach can be tricky when there are multiple generations of parent/child wells, plus the refracs, which have different stage lengths. To address this issue, sections of the model are 'cut out' of the model using a so-called 'zero-permeability cube.' An example is shown in Figure 5. The 'zero-permeability cube' approach is also useful for modeling production interference occurring between the outer well of the model and the 'next well over,' which is not included in the model. The 'zero-permeability cube' may be inactive during the fracturing period – allowing fluid to leak off along the full fracture lengths – and then activated during the production period avoid double-counting production.

Prior to the project, we hypothesized that the degree of 'crossflow outside casing' may be a significant 'tuning parameter' that assists in post-hoc matching of refrac data. By default, we assume that there is a fracture along the wellbore permitting crossflow, which is modeled having a height of 1 m and a conductivity of 10,000 md-ft. During model recalibration after unblinding, this conductivity was modified in order to match the actual post-refrac production data.

To evaluate the performance of the refrac and assess the quality of the model forecast, it was necessary to quantify the refrac uplift. The refrac uplift was computed for all datasets using Equation 1, where *Refrac Cum* is the refrac'd well's total oil cumulative (since the beginning of production) at a given time after the refrac. The *Forecast no refrac* is the estimated total oil cumulative production (since the beginning of production) at that same time without refrac. The forecast without refrac can be based on type curve analysis, DCA, RTA, or simulation.

$$Refrac\ uplift = \frac{Refrac\ Cum - Forecast\ no\ refrac}{Forecast\ no\ refrac} \quad \text{(Eq. 1)}$$

For example, let's assume that a well produced for seven years and had cumulative 400 Mbbl of production prior to the refrac. We estimate that at the end of year 8 – one year after the planned refrac – it would have reached a cumulative production of 430 Mbbl if a refrac had not been performed. Instead, with the refrac, it reached 580 Mbbl total production. In that case, the 'uplift' one year after the refrac is calculated as (580 – 430)/430 = 35%.

3. Results and discussion

Refrac predictions were performed for seven wells across four datasets – three from the Bakken and one from the Midland Basin. Most of the wells were originally completed with uncemented liner and relatively small fluid and proppant volumes. The refracs were performed by cementing a new liner inside the original liner, and by utilizing plug and perf with tighter cluster spacing and larger fluid and proppant volumes than the original design (Table 1, Table 2, Table 3, and Table 4).

Figure 1 shows a comparison between the blind simulation predictions and actual refrac uplift (defined in Equation 1) for each well after one year. For dataset BK3, only seven months of production were available post-refrac, and so the data was extrapolated to one year. Overall, the simulations were very effective at predicting performance, even though the datasets included a wide spread of outcomes. On average, after one year, the refracs achieved a 26% increase in the wells' cumulative production. The smallest increase was 10%, and the largest increase was 57%. The average mismatch in predicted uplift between the simulations and actual was 3.7%. A linear correlation through the data shows that the simulations tended to modestly underestimate actual performance. The r^2 of the regression line is 0.987.

At 1 year	Actual	Sim
BK1 1H	57%	52%
BK1 2H	49%	46%
MB1	20%	24%
BK2 E	21%	13%
BK2 G	11%	9%
BK2 I	15%	14%
BK3	10%	8%

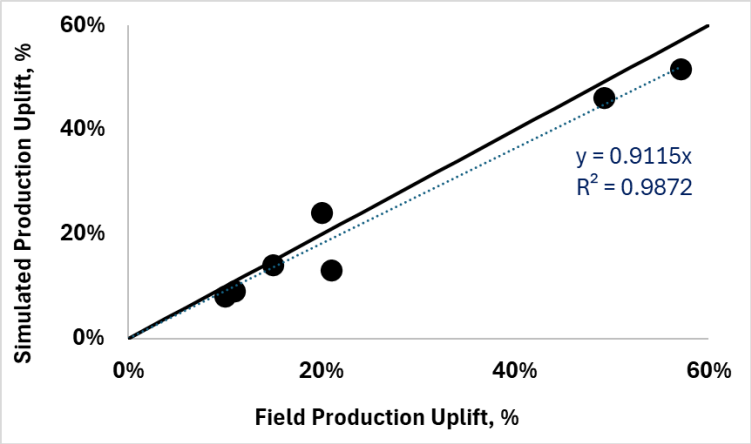

Figure 1. Crossplot of predicted versus actual refrac uplift (defined in Equation 1) at one year post-refrac. The solid black line shows equality, while the dashed line shows a linear regression through the data.

3.1 Dataset BK1

Figure 2 shows the gunbarrel configuration for Dataset BK1. Five wells were included in the simulation – Middle Bakken wells 1H and 2H, and Three Forks wells 3H, 4H, and 5H.

Well 4H was fractured and produced first. The other four wells were fractured 4.5 years later. The 1H and 2H were refractured 5.7 years after that, or 10.3 years after the original fracturing of 4H. In the original completions, Wells 1H, 2H, 3H, and 4H were completed with uncemented sliding sleeves; Well 5H was completed with cemented plug and perf and three clusters per stage. All wells except 4H used 320 ft stage length; the 4H used 480 ft stage length.

Table 1 compares the fracture designs. The original fracturing designs used relatively low fluid and proppant per ft of lateral.

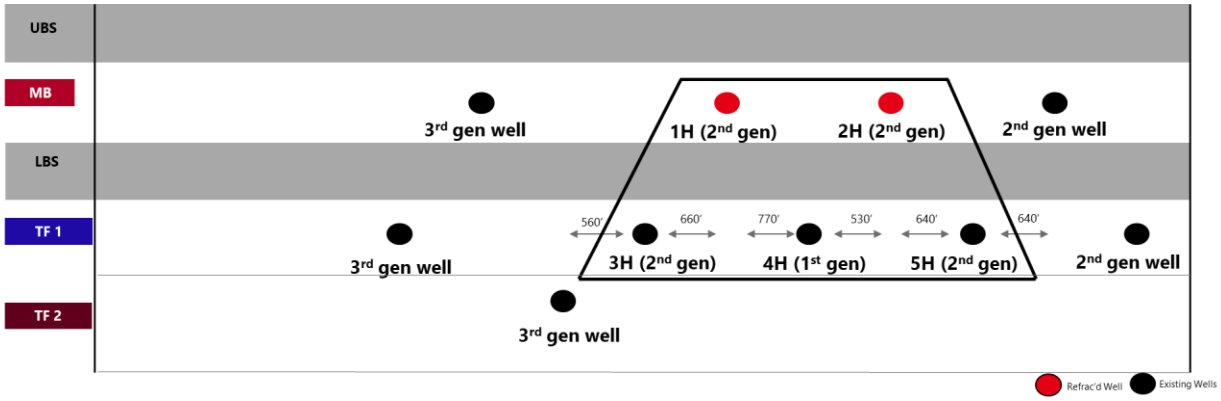

Figure 2. Well configuration in the BK1 dataset.

Table 1. Fracture design comparison for the five wells in the BK1 simulation.

Well Name	Zone	Completion Design		# Stages		Stage Length		# Entry points / Clusters		Fluid Loading		Proppant Loading		Main fracturing fluid	
		Primary	Refrac	Primary	Refrac	Primary	Refrac	Primary	Refrac	Primary	Refrac	Primary	Refrac	Primary	Refrac
1H	MB	Uncemented Sleeves	Cemented P&P	1x	1x	1x	1x	1x	8x	1x	3.5x	1x	2.8x	X-linked gel	Slickwater
2H	MB	Uncemented Sleeves	Cemented P&P	1x	1x	1x	1x	1x	8x	1x	3.5x	1x	2.8x	X-linked gel	Slickwater
3H	UTF	Uncemented Sleeves	-	1x	-	1x	-	1x	-	1x	-	1x	-	X-linked gel	-
4H	UTF	Uncemented Sleeves	-	0.66x	-	1.5x	-	1x	-	0.66x	-	0.66x	-	X-linked gel	-
5H	UTF	Cemented P&P	-	1x	-	1x	-	3x	-	1.5x	-	1.8x	-	X-linked gel	-

Relatively few field-scale diagnostics were available, and so the model was calibrated to ISIP observations and historical production. The latter provided indications of interference between wells, such as a boost in 4H oil rates after the completion of the offset wells and differences in production of up to 20% between neighboring co-developed wells. Historical production also indicated a mild difference in production between the two developed benches. These observations aided to partially constrain fracture geometry. For parameters affecting model behaviors such as fracture geometry and proppant pack conductivity, generic values were used, drawing on published values (Singh et al., 2025).

To calibrate the model, the following model inputs were modified: the stress profile, the number of fractures per stage in the uncemented sleeve completions, fracture toughness, permeability by zone, and relative permeability by zone.

In the initial simulation (prior to calibration), the Three Forks wells produced unrestricted from the Middle Bakken, causing the model to not reproduce the observation that Middle Bakken wells performed better. This was resolved by increasing the stress contrast between the layers and adding anisotropy of fracture toughness.

During the calibration process, it was decided to assume two fractures per stage in the uncemented liner wells, except in the 3H where a single fracture per stage was assumed. These assumptions allowed the model to replicate the boost in production in 4H after the primary completion of both MB wells without causing the performance in these wells to drop below the field data. Such behavior could not be accounted for by running the model with only one fracture per stage for all wells. Additionally, defining only one fracture per stage in 3H while modeling two fractures in TF allowed the model to match the 30% difference in oil cumulative between 4H and 3H in their first four years of production.

A set of ‘zero-permeability cubes’ were incorporated into the model to account for the difference in stage lengths between wells. Once activated, these cubes prevent further drainage from a set of specified zones, mimicking the interference of some portions of the longer stage in 4H with unmodeled shorter stages from its neighbor wells. These cubes are activated in the model immediately after the completion of the second-generation wells in year five.

Figure 3 and Figure 4 show the actual and simulated production before and after the refracs. The initial well, 4H, experienced a boost in production when the offset wells were fractured. This is reproduced in the simulation. The mismatch in production in 3H after 8.5 years is due to the completion of an unmodeled well to the west of the pad. Well 5H, which is the only well completed with plug and perf (albeit, with a much wider cluster spacing than is commonly used today), slightly outperformed its neighbors.

The model calibration was performed prior to reviewing the post-refrac production data. The ‘blind’ model prediction is quite good. Figure 4 shows that the simulation prediction and actual production in the 1H well match initially but then deviate sharply at roughly 1.75 years after the refrac. The deviation from trend occurred right after 1H transitioned from natural flow to an artificial lift system. This was an operational problem that could not have been anticipated by the blind simulation prediction.

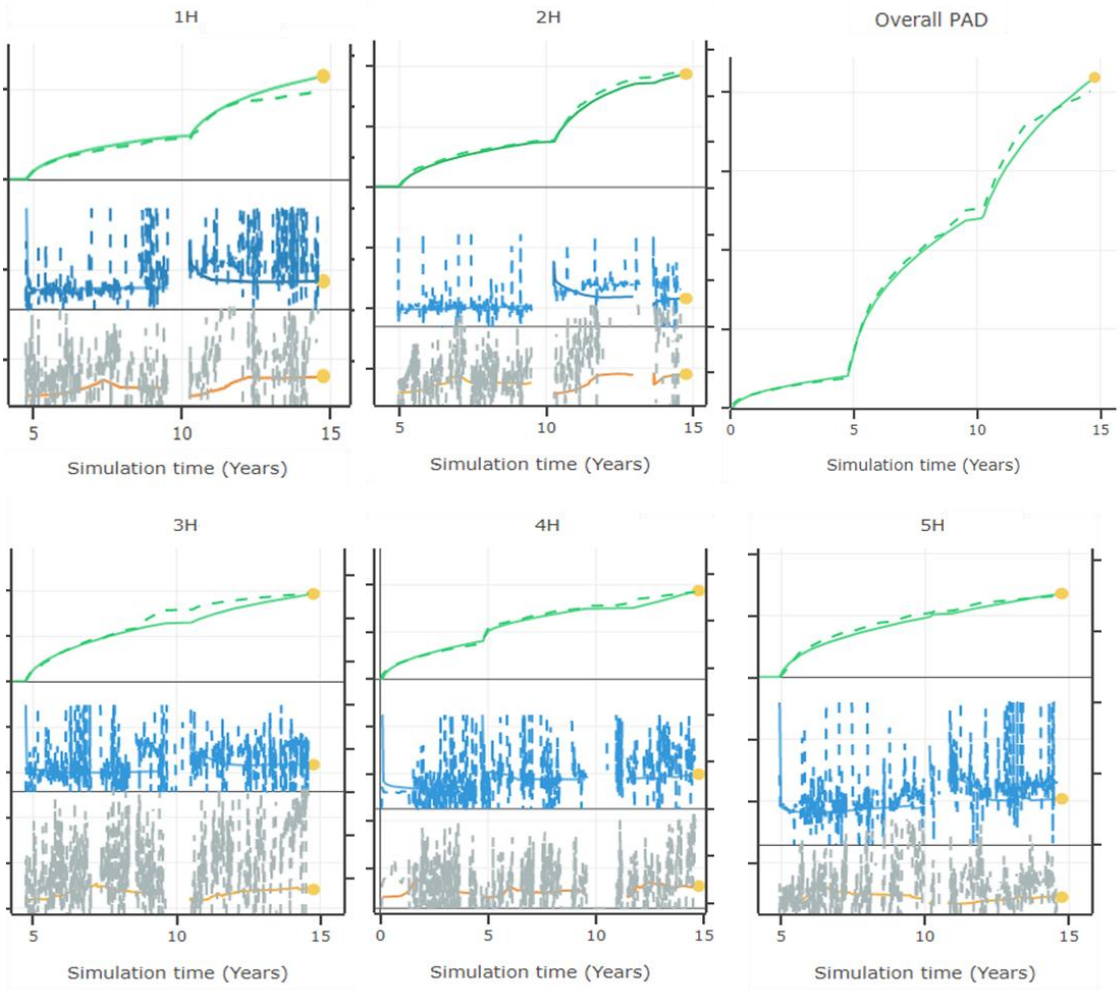

Figure 3. Comparison of actual (dashed) and simulated (solid) production in the BK1 dataset shortly before and after the refracs, including total oil in green, water cut in blue, and GOR in gray/orange.

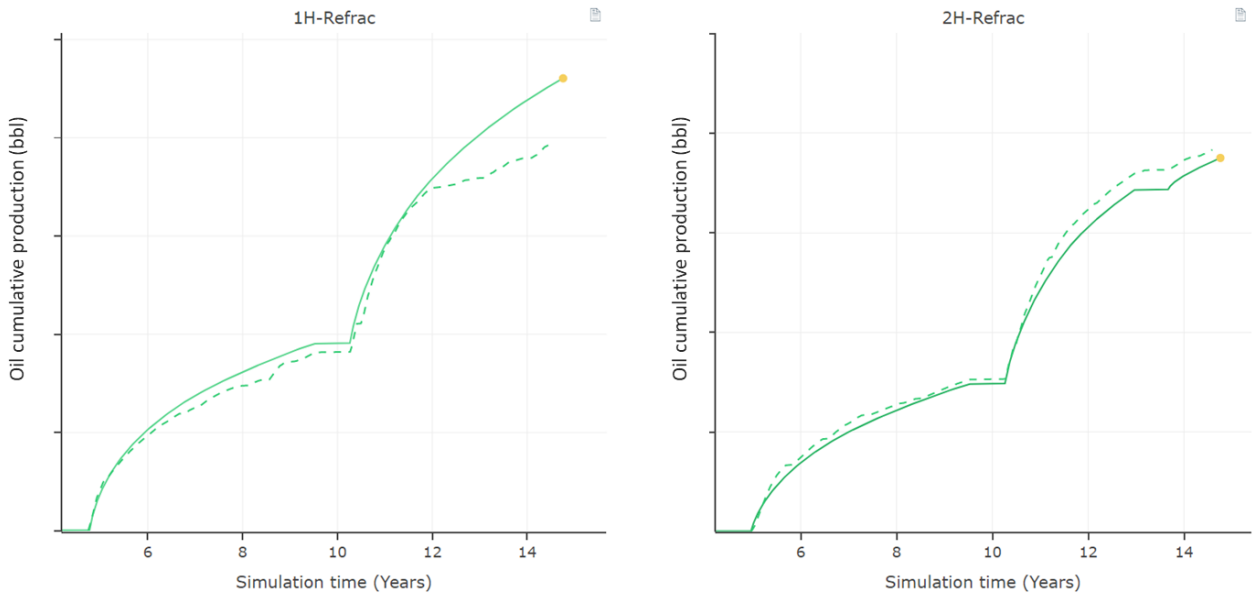

Figure 4. Comparison of actual (dashed) and simulated (solid) production in the 1H and 2H wells shortly before and after the refracs. The 1H actual production data deviates from trend 1.75 years post-refrac due to an issue with the artificial lift system.

Figure 5 shows the fracture geometries and depletion before and after the refracs. The refracs are effective because they fill-in gaps between the relatively widely spaced fractures from the original completions.

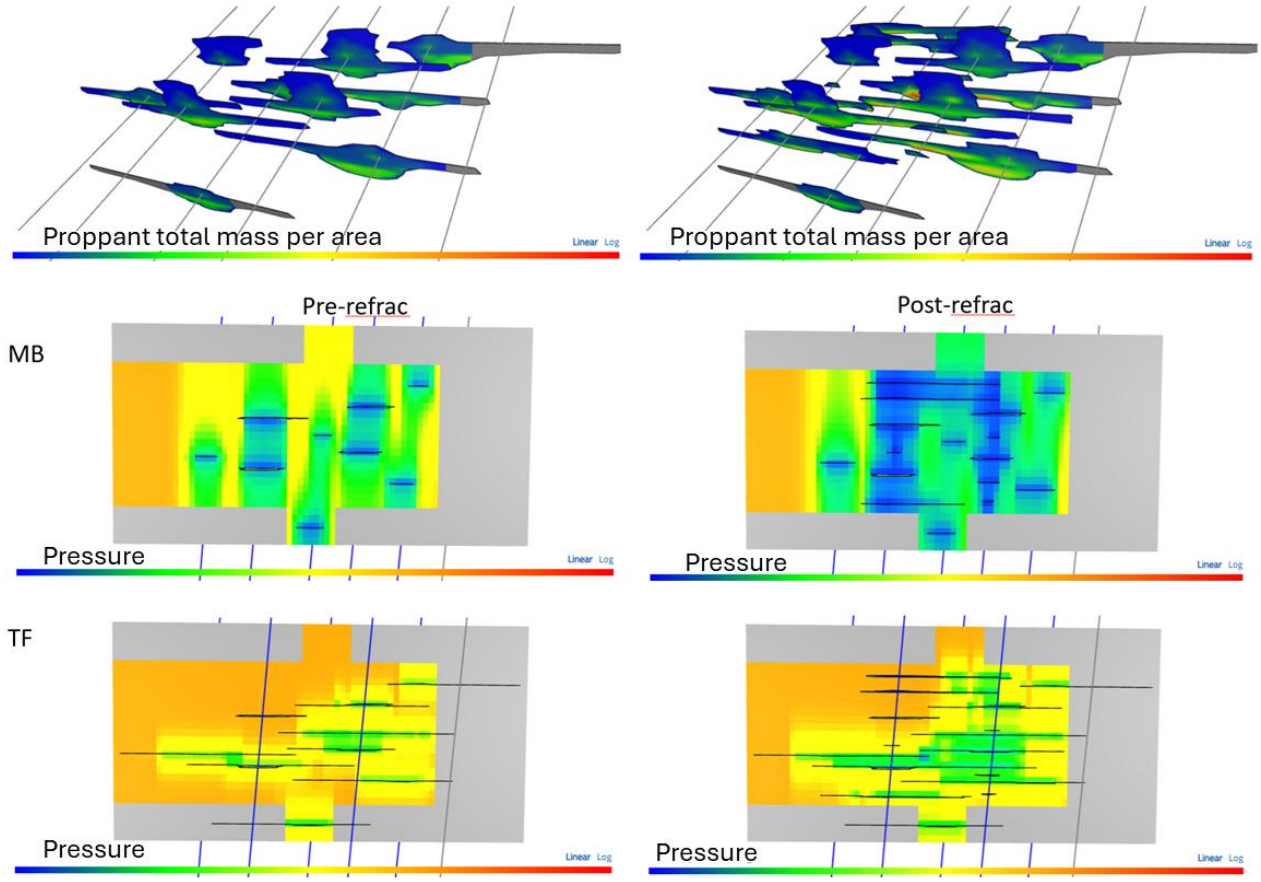

Figure 5. Comparison of fracture geometries and depletion before and after the refracs.

A second calibration step after comparing the blind predictions to actuals was envisioned. However, after comparing with the data, no model changes were necessary, because the match was deemed to be adequate.

Following Equation 1, the uplift of 1H was 57% one year after the refrac and 63% four years after the refrac. In comparison, the model predicted 52% and 82%, respectively. Running the model with greater BHP after year 12 (1.75 years after the refrac) to account for the problem in the artificial lift system brings down the uplift after four years to 63%, consistent with the actual data. In the case of 2H, the uplift in the field was 49% one year after the refrac and 67% four years after the refrac, while the model predicted 46% and 65%, respectively.

The simulation predicts that refracturing causes both re-stimulation of primary fractures and the creation of new fractures, some of which collide with depleted fractures from offset neighbor wells. The spatial drainage in MB and TF after the refrac was non-uniform, implying areas with variable drainage levels in both benches depending on the preferential growth of refrac fractures.

As a sensitivity, we decided to evaluate the effect of BHP versus time and well schedule following the refracs. Figure 6 shows the actual post-refrac well schedule, and then an alternative, simplified post-refrac well schedule. Figure 7 shows cumulative production versus time of the two scenarios. With the simplified BHP scenario, there is a substantial divergence in the per-well production results, even as the overall pad results remain similar. This comparison highlights the need for realistic BHP versus time and capturing the sequence that wells are put on production, to better predict individual well performance.

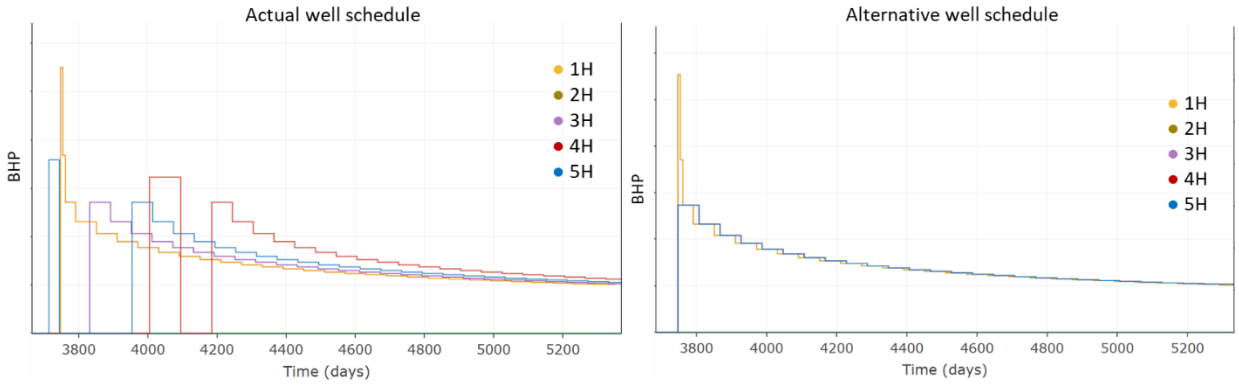

Figure 6. The actual BHP versus time schedule following the refrac (upper), and an alternative hypothetical well schedule (bottom).

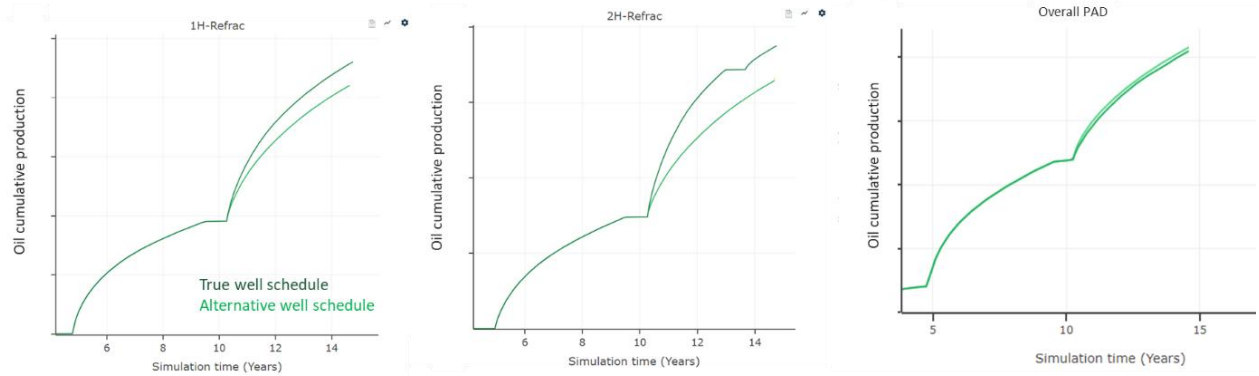

Figure 7. Production versus time for the 1H, 2H, and the overall pad if the model assumes an alternative (incorrect) well schedule following the refracs.

After the comparison was performed, the operator requested a model update and rematch using an alternative stress profile with lower stress in the Lower Bakken. The new stress profile yielded moderately shorter fracture lengths. To account for this difference in the fracture geometry, the number of entry points per stage in wells with sliding sleeve completion was increased from 1-2 in the initial model to 2-3 in updated model. Additionally, the overall permeability of the model was reduced by 30%. The model was calibrated solely to the pre-refrac data and then compared with the post-refrac data. As with the original match, the refrac uplift was predicted with good accuracy. Of course, in this second version of the model, the actual refrac performance was not 'blind,' since the model updates were performed after the actual refrac performance had been provided by the operator. Figure 8, Figure 9, and Figure 10 display the results from the updated model.

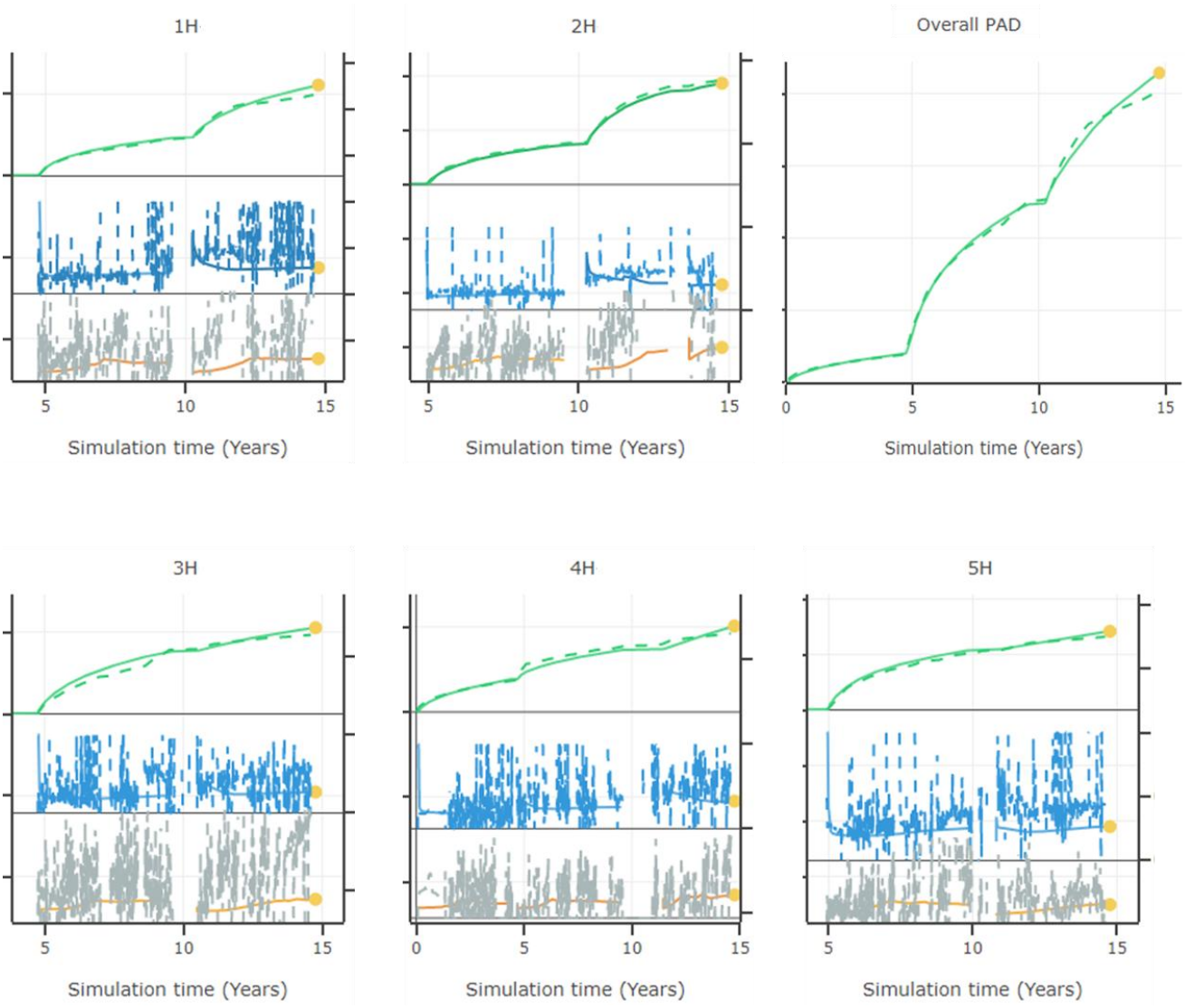

Figure 8. Comparison of actual (dashed) and simulated (solid) production in the BK1 model (using the updated stress profile) shortly before and after the refracs, including total oil in green, water cut in blue, and GOR in gray/orange.

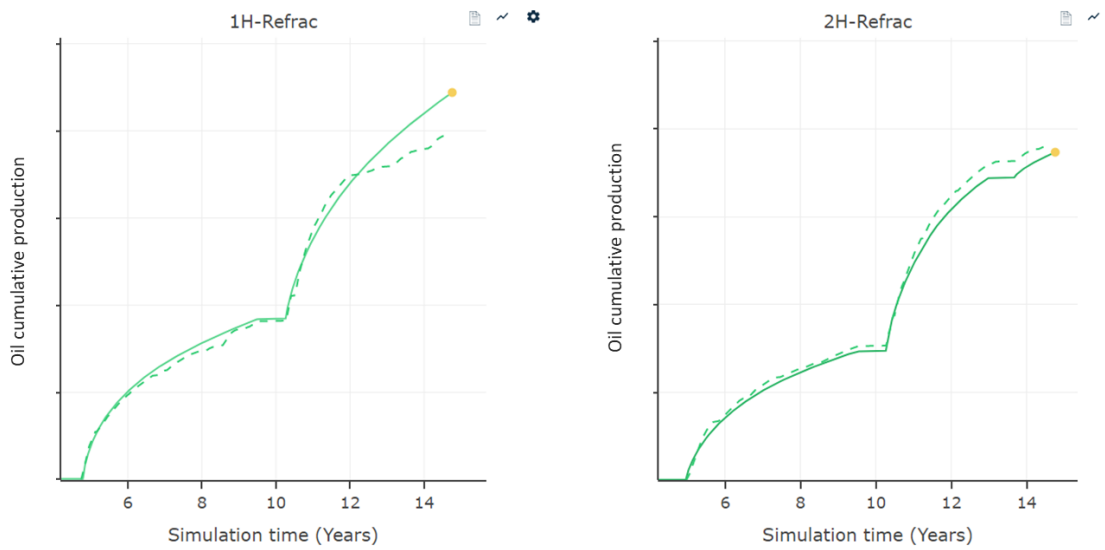

Figure 9: Comparison of actual (dashed) and simulated (solid) production in the 1H and 2H wells shortly before and after the refracs in the BK1 model recalibrated with the updated stress profile. The 1H actual production data deviates from trend 1.75 years post-refrac due to an issue with the artificial lift system.

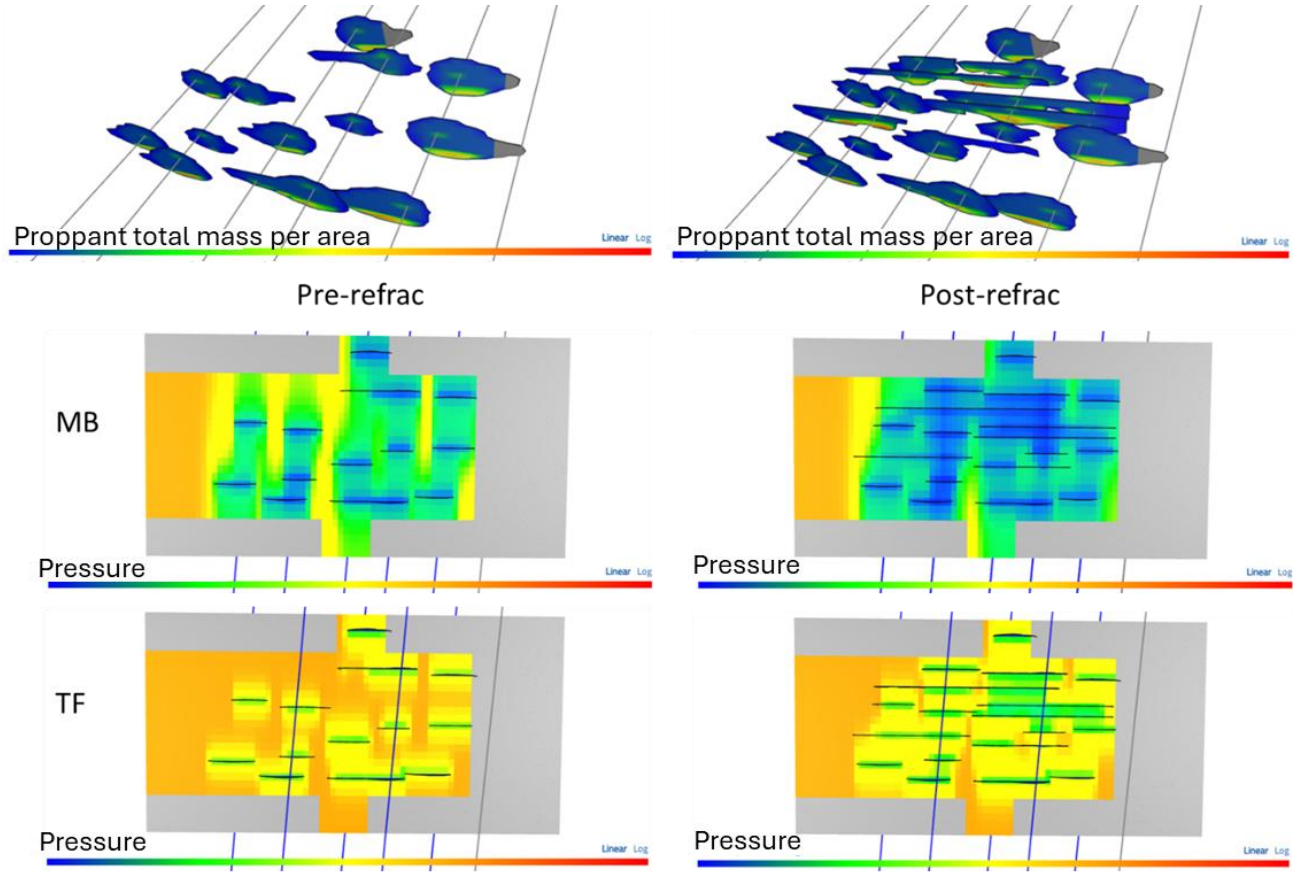

Figure 10. Comparison of fracture geometries and depletion before and after the refracs from the BK1 model recalibrated with a different stress profile.

Figure 10 shows that depletion is somewhat more uniform in the updated model compared to the original one (Figure 5) because of the presence of more fractures created during the primary completion before the refrac. The predicted uplift in the re-calibrated model is 48% in 1H and 47% in 2H after the first year of production, against 57% and 49%, respectively in the real data. After four years of production and without accounting for the issues in the artificial lift system in 1H, the model uplift reaches 77% in 1H and 65% in 2H, while the real data showed 63% in 1H and 67% in 2H. If the model is re-run with greater BHP in 1H after 1.75 years since the start of the refrac to account for the artificial lift issue, the simulated uplift in 1H goes down to 67%.

The recalibration exercise shows that because of the 'model calibration' step, the prediction of overall refrac performance remains robust, despite uncertainty and non-uniqueness in the details of the static model.

3.2 Dataset BK2

In this dataset, four Middle Baken wells were refractured (Well A, E, G, and I). The gunbarrel configuration is shown in Figure 11. The simulation model includes only the five wells to the left – Well E to Well I.

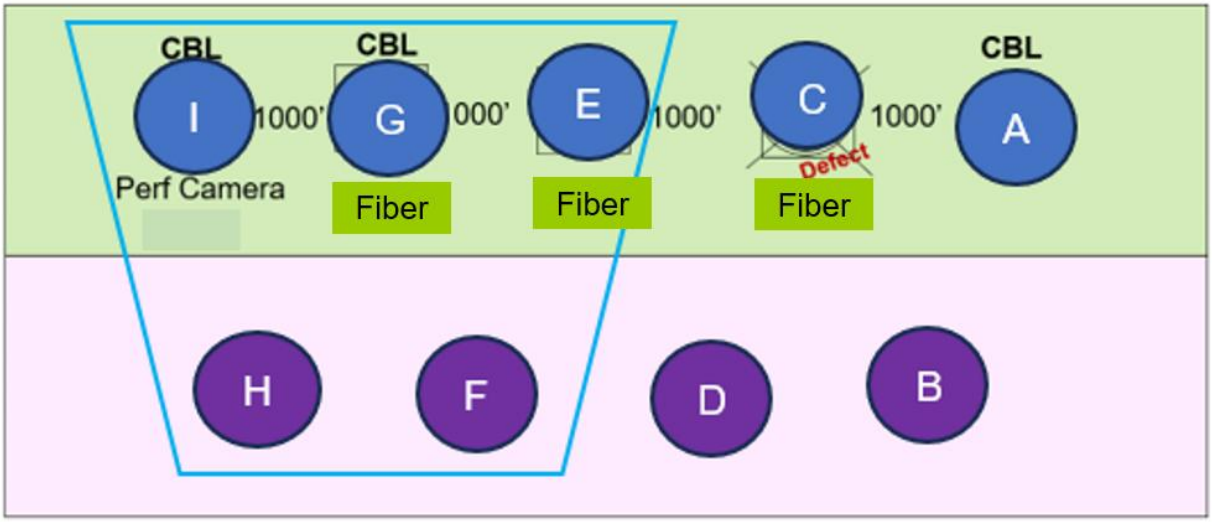

Figure 11. Well configuration in the BK2 dataset.

The wells were originally fractured with uncemented sliding sleeve completions. Relative to more recent Bakken stimulations, the original fluid and proppant volumes were low on a per ft of lateral basis (Table 2). The refracs were performed by cementing a new liner and injecting around 2.5 - 3x more fluid and proppant per ft than the original completions, at a 30-37 ft cluster spacing. The refracs were performed roughly nine years after the original completions. Refrac diagnostics include fiber optics, cement bond log (CBL), downhole perforation imaging, and sealed wellbore monitoring.

Table 2. Fracture design comparison for the five wells in the BK2 simulation.

Well Name	Zone	Completion Design		# stages		Stage Length		# Entry Points/Cluster		Fluid Loading		Proppant Loading		Fracturing Fluid	
		Primary	Refrac	Primary	Refrac	Primary	Refrac	Primary	Refrac	Primary	Refrac	Primary	Refrac	Primary	Refrac
E	MB	Uncemented Sleeves	Cemented P&P	1X	1X	1X	1X	1X	10X	1X	3X	1X	2X	Crosslinked	HVFR
F	UTF	Uncemented Sleeves		1X		1X		1X		1X		1X		Crosslinked	
G	MB	Uncemented Sleeves	Cemented P&P	1X	1X	1X	1X	1X	10X	1X	3X	1X	2X	Crosslinked	HVFR
H	UTF	Uncemented Sleeves		1X		1X		1X		1X		1X		Crosslinked	
I	MB	Uncemented Sleeves	Cemented P&P	1X	1X	1X	1X	1X	10X	1X	3X	1X	2X	Crosslinked	HVFR

The calibration process started with an existing model (which was previously described by Singh et al., 2025). The formation properties and model inputs were all left unchanged. However, some calibration to match the pre-refrac well production was necessary. This was performed by varying the number of fractures

propagating from each uncemented stage during the original stimulations. This was varied because, as discussed in Section 2, the number of newly propagating fractures from an uncemented stage is not well-constrained. As part of the calibration, the wells were given either two or three fracture initiation points.

Model calibration was accomplished solely by varying fracture initiation points, and no other parameters. The matched data included: volume to first response during the refracs, treating pressures and ISIPs, the well production (including that the Three Forks wells underperform the Middle Bakken wells by 18%), downhole imaging-based erosion measurements taken after the refracs.

Figure 12 and Figure 13 show the pressure drawdown in the Middle Bakken and Three Forks before the refracs and one year after the refracs. The images show that there are substantial regions that remain undepleted. Even following the refracs, there are significant gaps in the depletion. This is probably because the refracs – while larger than the original fracs – were still relatively small in volume on a per-cluster basis, and so they did not create pervasive new fractures throughout the formation. In addition, a significant percentage of fluid and proppant flowed back into the original fractures.

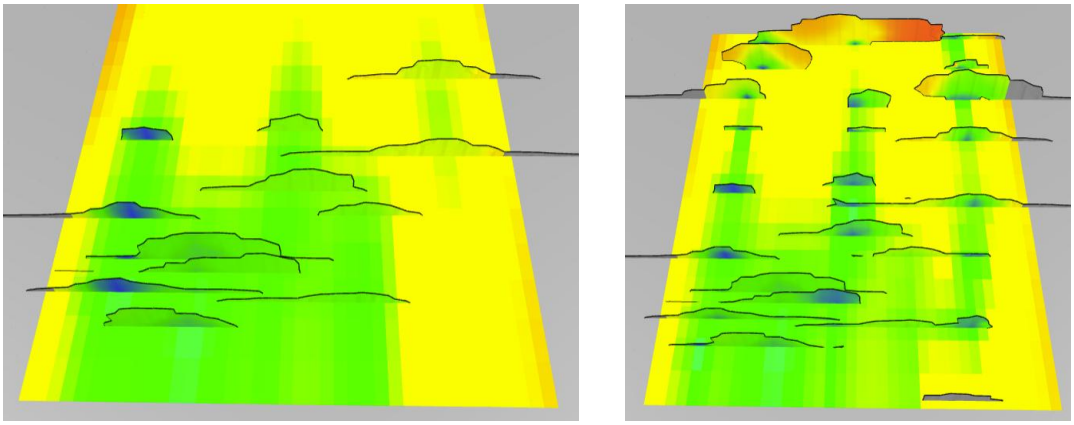

Figure 12. Pressure drawdown in the Middle Bakken prior to the refracs (left) and one year after the refracs (right).

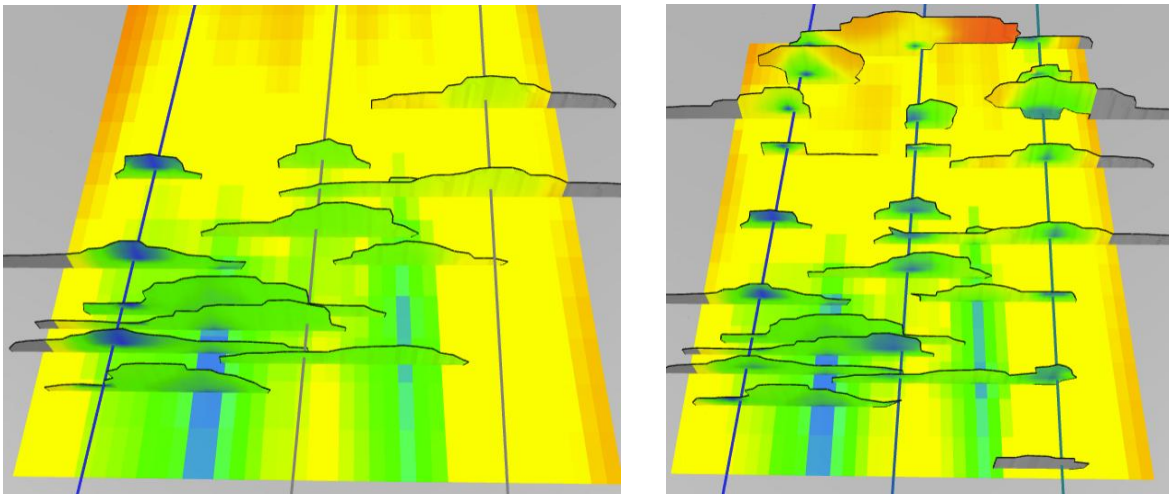

Figure 13. Pressure drawdown in the Three Forks prior to the refracs (left) and one year after the fracs (right).

Figure 14 shows the actual and simulated production for the Middle Bakken refrac'ed wells, including the period following the refracs. Figure 15 shows the actual and simulated production for the Three Forks wells

– which were not refrac'ed. Figure 16 shows the combined production of the five wells before and after the refracs.

As with the other datasets, the simulation match was performed solely to the pre-refrac data. The unblinded comparison with the post-refrac production is fairly good. Figure 15 and Figure 16 show the impact of the refracs on the individual well production. In the actual data, the wells showed an uplift of 21%, 11, and 15% (average of 15%) after one-year post-refrac; the blind predictions were 13%, 9%, and 14% (average of 12%). In both the simulations and actual data, the Three Forks wells showed a minor increase in their productivity due to Middle Bakken offset wells' refracs in the range of 2% - 3% two-years post refrac. Following comparison with the blinded refrac results, we chose not to make any further adjustments to the model.

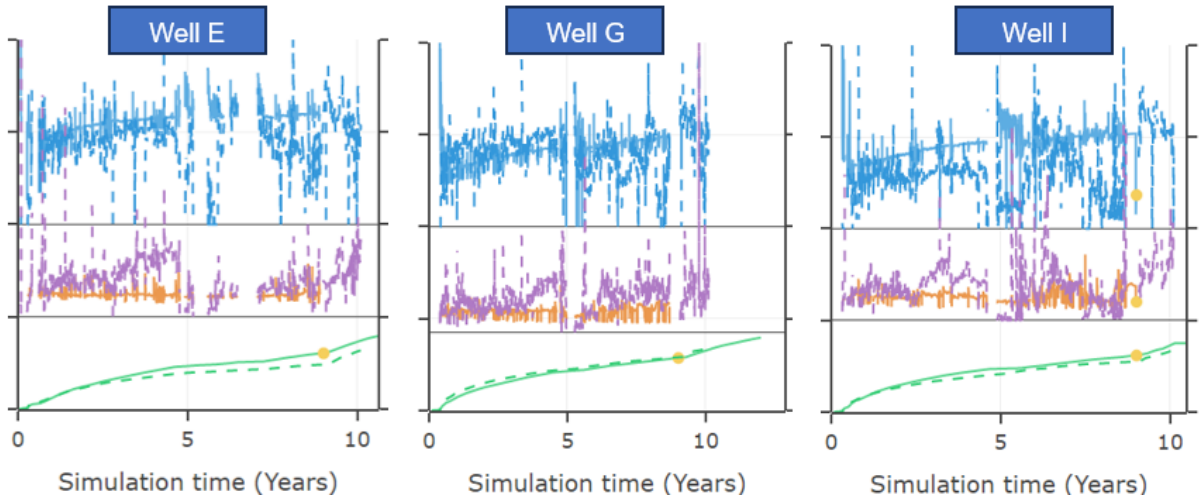

Figure 10. Production history matching of the refrac'ed Middle Bakken wells pre and post refrac, including total oil matching in green, water cut matching in blue, and GOR matching in orange – model is in solid and actual data in dashed lines.

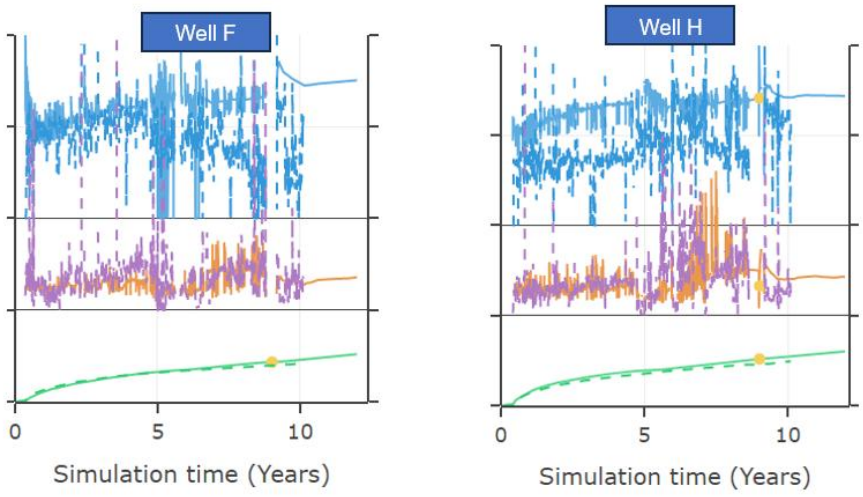

Figure 11. Production history matching of the non refrac'ed Three Forks wells pre and post refrac, including total oil matching in green, water cut matching in blue, and GOR matching in orange - model is in solid and actual data in dashed lines.

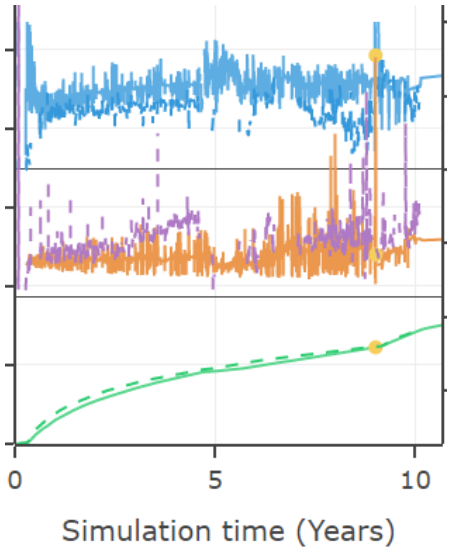

Figure 14. Sector model history matching pre and post refrac, including Middle Bakken and Three Forks wells, including total oil matching in green, water cut matching in blue, and GOR matching in orange - model is in solid and actual data in dashed lines.

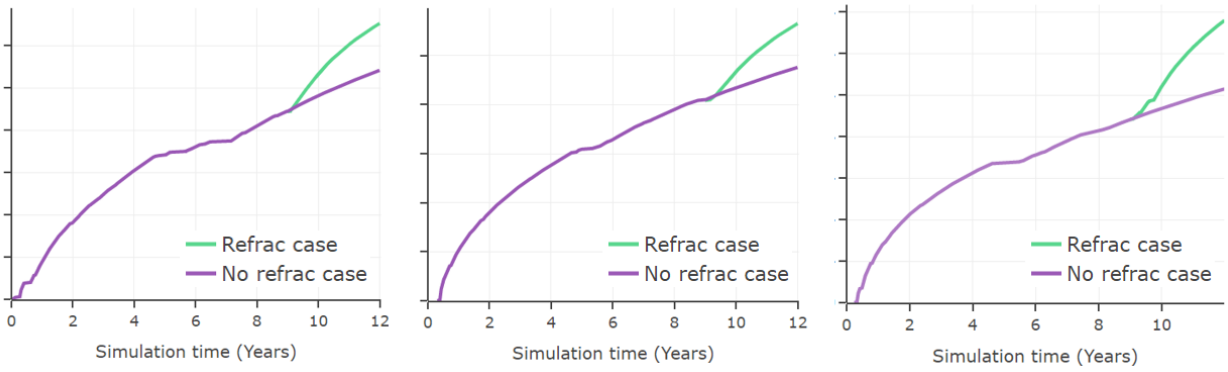

Figure 15. Middle Bakken wells total oil production uplift from the refracs (simulated data).

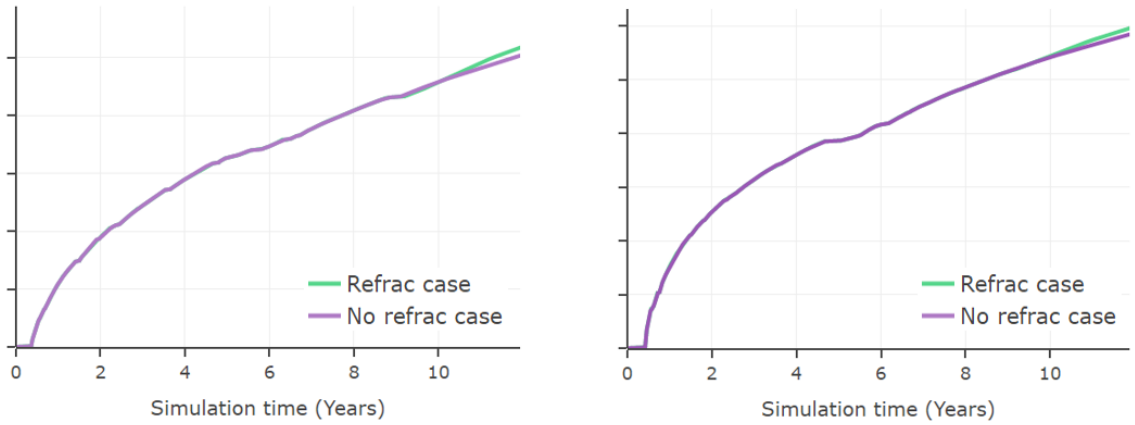

Figure 16. Three Forks wells total oil production uplift from the Middle Bakken offset wells refracs (simulated data).

3.3 Dataset BK3

Dataset BK3 includes only a single refrac well, a Middle Bakken well that was originally completed in 2013. There are several generations of wells, as shown in Figure 17 and Figure 18. All of the completions used plug and perf. The 1st and 2nd generation wells used uncemented liners. The 3rd generation wells A and B used cemented plug and perf with substantially larger fluid and proppant volumes and tighter cluster spacing. The 1st generation wells were fractured with 20/40 and 40/70 proppants and crosslinked gel. The subsequent fracs were a mixture of HVFR and slickwater with 40/70 and 100 mesh. The cluster spacing decreased from 57 to 30 ft, from the oldest to newest fracs.

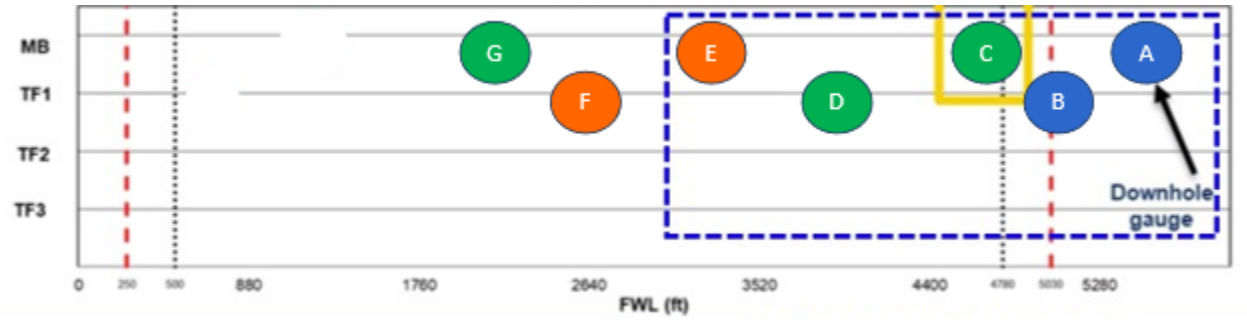

Figure 17. Gunbarrel configuration for the wells in Dataset BK3. 1st generation wells are shown in green, 2nd generation wells are shown in orange, and 3rd generation wells are shown in blue. The simulation included the wells within the dashed blue box.

- 1st generation TF well D underperforms MB well C by 22%
- 3rd generation TF well B underperforms MB well A by 6%
- 2nd generation MB well E outperforms the first and third generations wells due to the bigger frac
- The MB well C produced about 265k STB prior to refrac

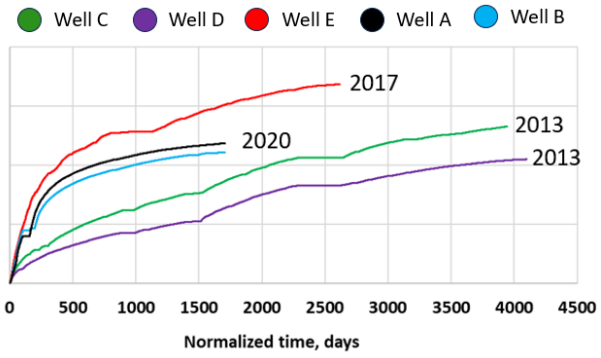

Figure 18. Comparison of cumulative oil production versus time for the different generations of wells in Dataset BK3.

Table 3. Fracture design comparison for the five wells in the BK3 simulation.

Well Name	Zone	Completion Design		# stages		Stage Length		# Entry Points/Cluster		Fluid Loading		Proppant Loading		Fracturing Fluid	
		Primary	Refrac	Primary	Refrac	Primary	Refrac	Primary	Refrac	Primary	Refrac	Primary	Refrac	Primary	Refrac
A	MB	Cemented P&P		1.43X		0.67X		2.33X		3.8X		4.2X		HVFR	
B	UTF	Cemented P&P		1.47X		0.69X		2.33X		2.8X		2.8X		HVFR	
C	MB	Swellable Packers P&P	Cemented P&P	1X	0.9X	1X	1.11X	1X	2.7X	1X	3X	1X	3.5X	Crosslinked	Slickwater
D	UTF	Swellable Packers P&P		1X		1X		1X		0.86X		1X		Crosslinked	
E	MB	Swellable Packers P&P		1.97X		0.5X		1.33X		3.9X		3.6X		Crosslinked	

Model calibration was based on microseismically-derived measurements of fracture height growth, ISIPs, and production data. Fracture height growth for the parent wells was validated using microseismic from a nearby, similarly designed pad of the same vintage. The microseismic suggested no height growth up into the Lodgepole. In some Bakken datasets, height growth is observed up into the Lodgepole (Singh et al., 2025). However, the stress profile is variable across the basin, and in this area, the microseismic data provides confidence that the stress profile prevents growth into the Lodgepole.

Figure 19 shows the fracture geometry and proppant from the calibrated model for BK3. Figure 20 shows the actual and simulated production from the wells in the model. Most wells exhibit a close match. Although, Well B is modestly underpredicted by the model and Well D is modestly overpredicted.

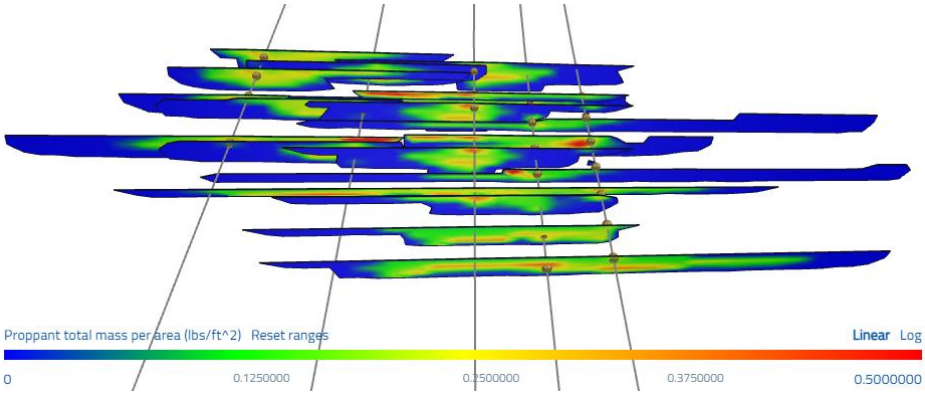

Figure 19. Fracture geometry and proppant placement before refrac from Dataset BK3.

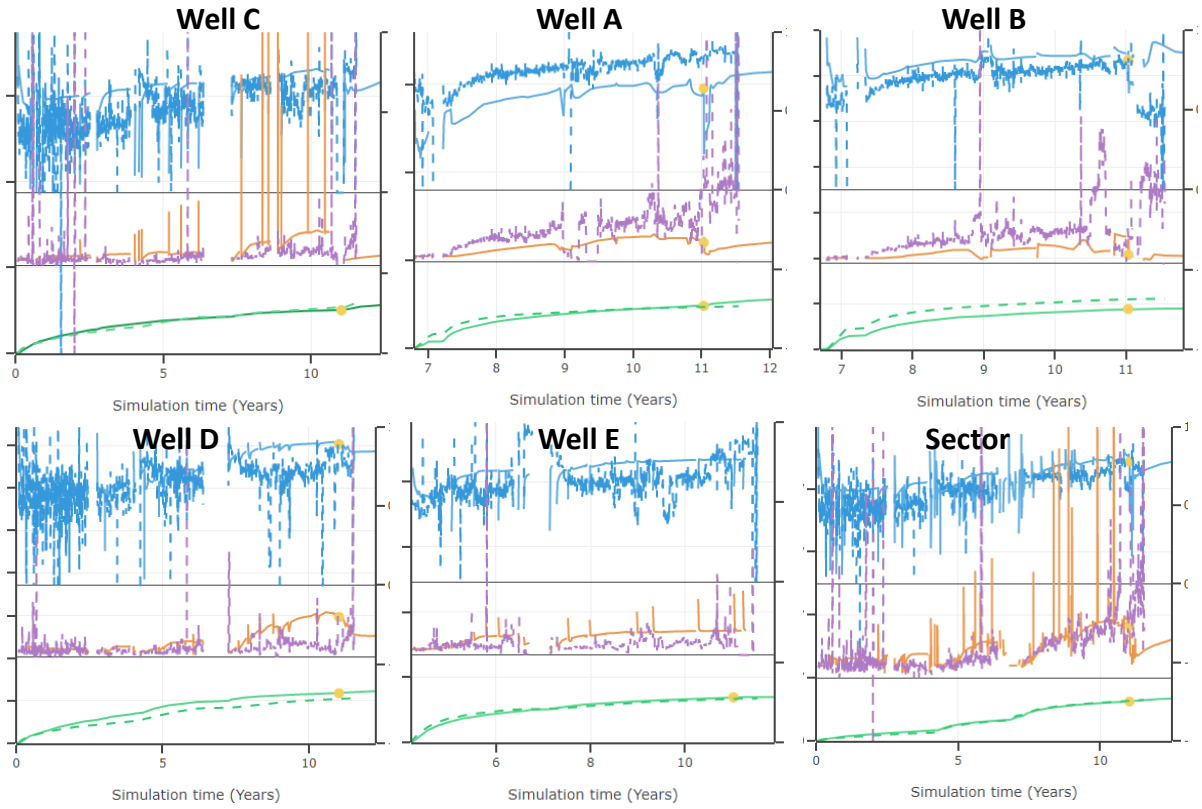

Figure 20. Production history matching of all wells and sector pre and post refrac, including total oil in matching in green, water cut matching in blue, and GOR matching in orange - model is in solid and actual data in dashed lines.

Figure 21 shows the simulated and actual production before and after the refrac. As with the other datasets, the simulation prediction was made prior to reviewing the actual post-refrac data. In this case, the model prediction trends somewhat below the actual production. Prior to the refrac, the simulation was already trending slightly below the actual observed production. Therefore, to normalize, the right panel of Figure 21 shows the actual and simulated production post-refrac.

On an absolute basis, the uplift from the refrac was low. At one year, the extrapolated uplift was only 10%, the lowest of any well in this study. The blind model prediction correctly predicted the underperformance of the BK3 refrac, relative to the other datasets, although it was moderately too pessimistic.

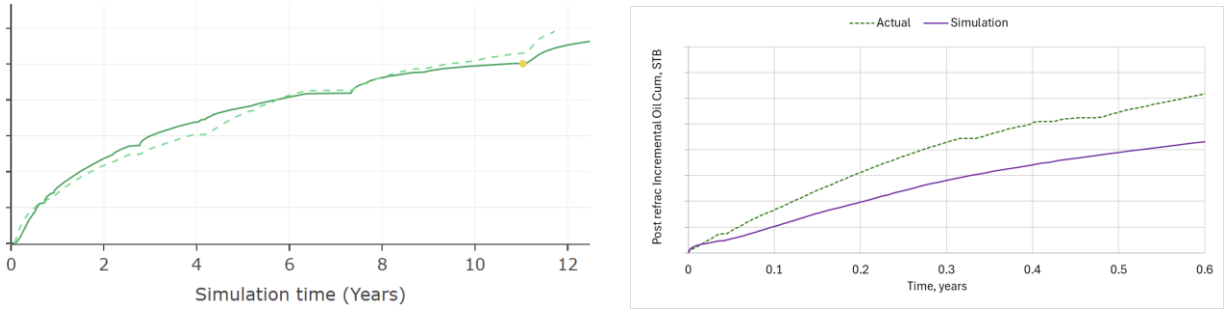

Figure 21. Actual (dashed) and simulated (solid) total oil production for Well C before and after the refrac (left) and the actual and simulated post-refrac production (right).

The BK3 refrac seems to have underperformed relative to other datasets because Well C was surrounded by wells that were fractured with relatively modern high-density fracture designs, leaving less unproduced oil. Figure 22 shows the distribution of pressure depletion prior to the 3rd generation child wells four years prior to the refrac, immediately prior to the refrac, and two-years post-refrac. Because of the high density fracturing from the 3rd generation wells, the pressure depletion is strong, with most of the Middle Bakken depleted prior to the refrac (middle panel). Figure 23 shows the distribution of frac fluid during the refrac. Some new fracture surface area is being created, but most of the frac fluid is reinflating the densely-spaced preexisting fractures.

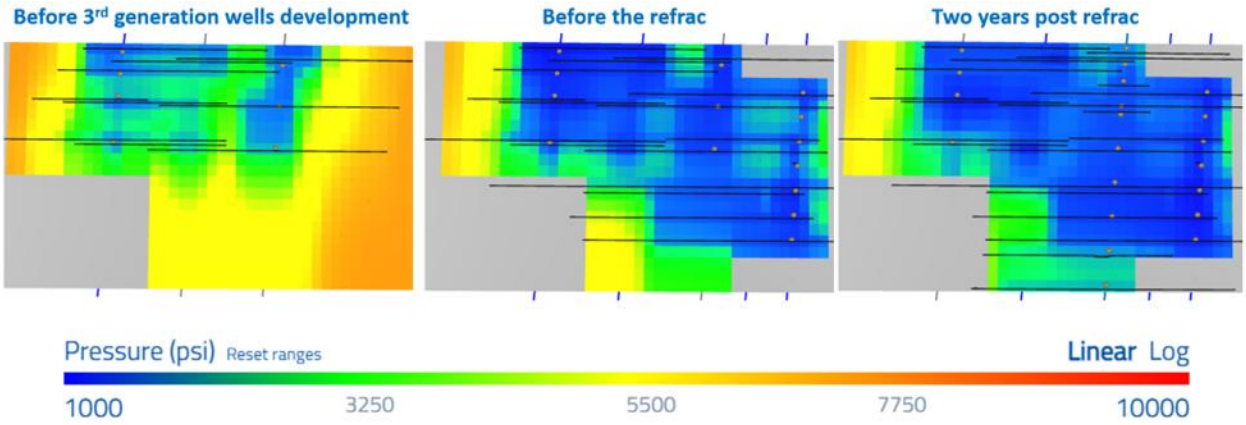

Figure 22. Distribution of pressure depletion in the Middle Bakken prior to the 3rd generation child wells, prior to the refrac, and two years post-refrac.

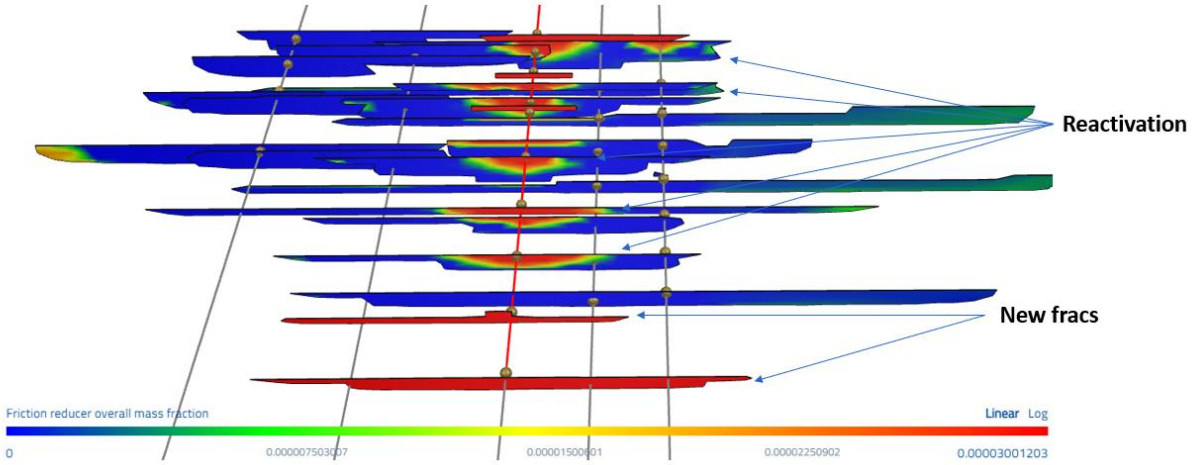

Figure 23. Plot showing the concentration of frac fluid friction reducer during the refrac. It shows a combination of newly forming fractures and reactivation of preexisting fractures.

To quantify the effect of the high-density 3rd generation fracs around the refrac, a hypothetical simulation was performed in which the refrac was performed shortly before the 3rd generation wells, instead of several years after. Figure 24 shows the result. Without the prior depletion of the nearby 3rd generation wells, the refrac uplift was much greater – around 55% one-year post refrac.

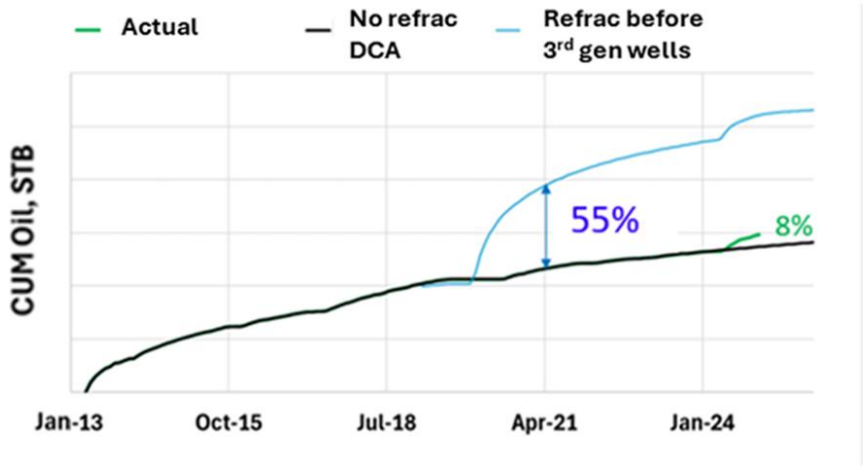

Figure 24. Production uplift under two scenarios; (a) when refrac was done after 3rd generation wells development (green), and (b) when refrac is done prior to 3rd generation wells development (blue).

Following comparison with the blinded results, the model inputs were adjusted to improve the match (Figure 25). To increase the predicted performance following the refrac, the amount of crossflow was reduced by changing the conductivity for crossflow from 10,000 md-ft to 1000 md-ft. This change alone was sufficient to achieve a reasonable match, as shown in Figure 25.

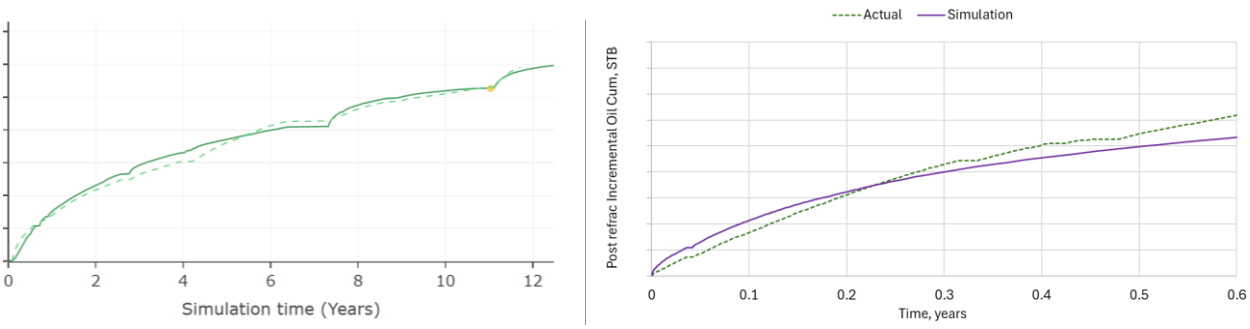

Figure 25. Actual (dashed) and simulated (solid) total oil production for Well C before and after the refrac (left) and the actual and simulated post-refrac production (right). The simulation shows the unblinded recalibration to the refrac data, which was accomplished by decreasing the magnitude of crossflow outside casing.

3.4 Dataset MB1

This dataset involves a single Midland Basin Wolfcamp well that was refractured three years after its initial completion. This dataset has six years of post-refrac production data available. The well was initially unbounded on both sides. An offset well child well was completed simultaneously with the refrac but not included in this study.

Table 4. Fracture design comparison for the wells in the MB1 simulation.

Well Name	Zone	Completion Design		# stages		Stage Length		# Entry Points/Cluster		Fluid Loading		Proppant Loading		Fracturing Fluid	
		Primary	Refrac	Primary	Refrac	Primary	Refrac	Primary	Refrac	Primary	Refrac	Primary	Refrac	Primary	Refrac
A	WC	Cemented P&P	Cemented P&P	1X	1.86X	1X	0.5X	1X	2.75X	1X	2.10X	1X	0.56X	Crosslinked	Slickwater

As with Dataset BK1, the starting point was a simulation model that had been previously built as part of a prior study (Singh et al., 2025). To calibrate to the primary production of this particular dataset, minor changes were made to proppant related parameters – the ‘maximum immobilized proppant trapping’ (a parameter that affects the size of the propped area), the proppant conductivity, and the fluid system viscosity (which was considered uncertain, based on the available data from the original frac). Also, while the post-refrac production data was not provided, the pressure versus time pumping data from the refracs *was* provided for the calibration. This was useful because the refracs utilized diverter, and we wanted to be able to calibrate to the pressure responses that were observed in response to the diverter drops. Without any calibration for a particular diverter system, it can be difficult to be predictive because of the variability that exists in diverter performance.

Figure 26 and Figure 27 show the actual and simulated production for the well. The simulation was history matched solely to the production data prior to the refrac. The simulations did a good job of predicting the refrac performance, with a slight overprediction.

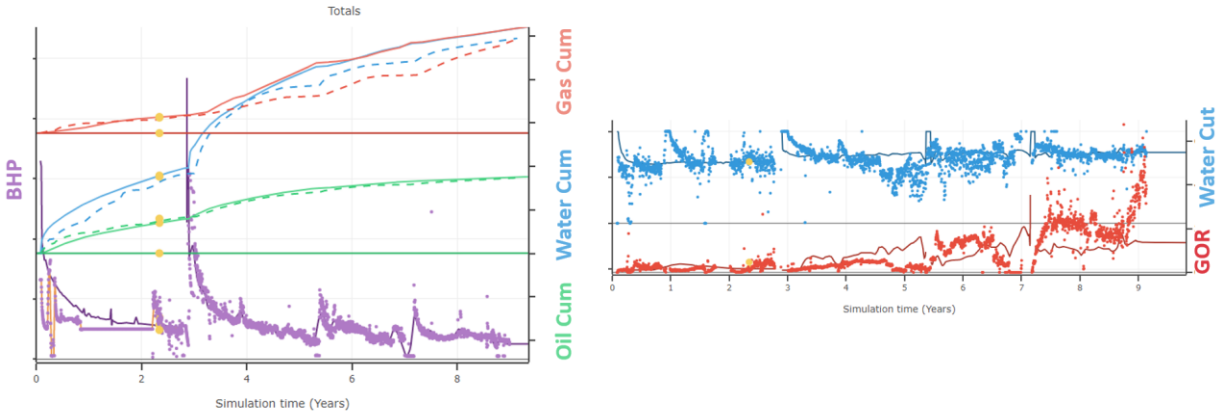

Figure 26. Actual (dashed) and simulated (solid) production for the Wolfcamp well from the MB1 dataset. The simulation predictions were made based on a history match to solely the data prior to the refrac.

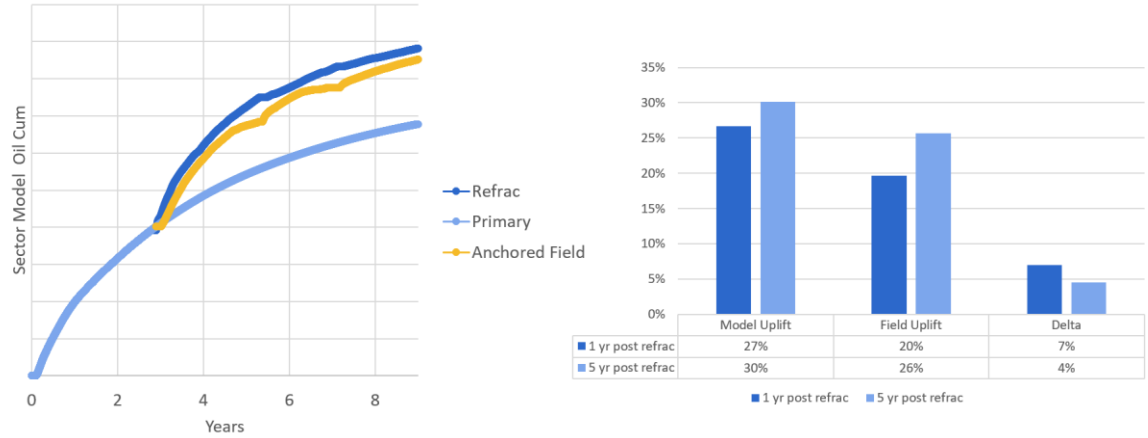

Figure 27. Actual (gold) and simulated (dark blue and light blue) production for the Wolfcamp well from the MB1 dataset. The simulation predictions were made based on a history match to solely the data prior to the refrac.

Figure 28 and Figure 29 show the pressure distributions around the fractures before and after the refrac. The original cluster spacing was relatively wide, leaving substantial undrained rock between the fractures. The refrac significantly fills in the gaps, resulting in substantially better recovery.

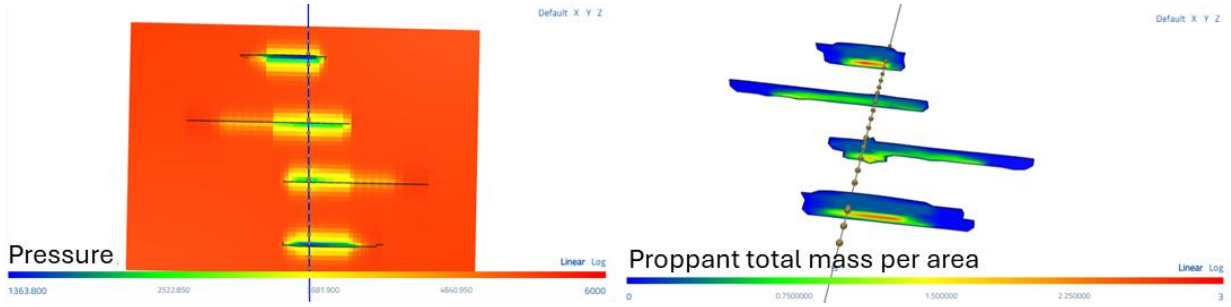

Figure 28. Pressure and proppant placement in the MB1 simulation prior to the refrac.

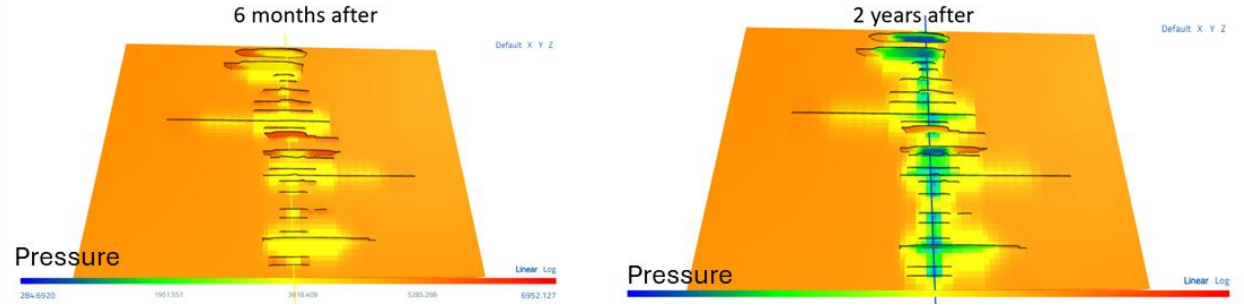

Figure 29. Pressure distribution six months and two years after the refrac.

Figure 30 shows the distribution of frac fluid at two different points in time during the refrac. As in the other simulations, there is a moderate amount of crossflow back into the original fractures.

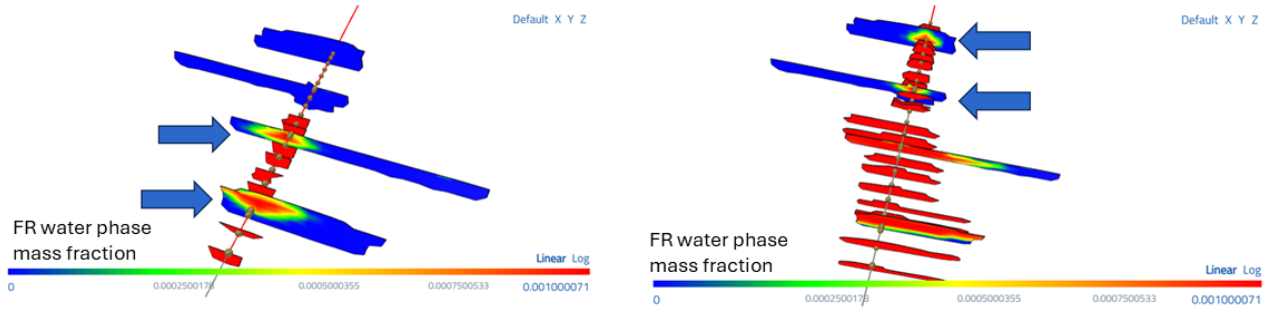

Figure 30. Frac fluid distribution at two different points during the refrac.

Following comparison with the post-refrac data, it was found that the match could be improved by modestly reducing the assumed efficacy of the diverter and by increasing the amount of crossflow into the original fractures by increasing the ‘conductivity for flow outside casing’ to 100,000 md-ft (up from the default value of 10,000 md-ft).

4. Conclusions

The blind refrac predictions had good accuracy. On average, after one year, the refracs achieved a 26% increase in cumulative production. The smallest increase was 10%, and the largest increase was 57%. The average mismatch in predicted one-year refrac uplift was 3.7%.

The simulations confirm our intuition that wells that have been understimulated – and that have understimulated neighbors – can be strong refrac candidates. However, if adjacent neighbors have been stimulated with high-density fracturing, refractured wells can experience relatively low uplift.

Prior to the project, we had hypothesized that the degree of 'crossflow outside casing' may be a significant 'tuning parameter.' In fact, with post-hoc calibration to known refrac production data, we did find that varying this parameter could improve the match to refrac data. In two datasets, no further recalibration was justified. However, in one dataset, we were able to improve the match by making the conductivity for crossflow 10x higher, and in another dataset, we made it 10x lower. Overall, we conclude that the baseline value of 10,000 md-ft should continue to be used as a 'default.' To estimate the hi/low range of potential outcomes, sensitivities can be run with this parameter in the range from 1000 and 100,000 md-ft.

In future work, we will perform optimization of refrac design for each dataset. Even though refrac performance varies widely between wells, the simulation results show that this variability is predictable. This gives us the ability to screen candidates and optimize performance.

Acknowledgements

We gratefully acknowledge the support of APA Corporation, ConocoPhillips Corporation, Continental Resources, Devon Energy, ExxonMobil Corporation, and Hess Corporation. Thank you to our colleagues who provided helpful feedback on the manuscript.

References

Barba, Robert E. 2024. A Comparison of Petrophysically Derived Post Refrac Recoverable Oil and Gas with Offset New Well EUR Results. Paper URTeC-4042322 presented at the Unconventional Resources Technology Conference, Houston, TX.

Brinkley, Kourtney, Cameron Thompson, Jackson Haffener, Sarah White, Chris Ketter, Jarret Borell, Joe Comisky, Eric Hart, Kyle Haustveit, Matthew Herrin, Peter Jones, Kevin Pelton, Ken Pfau, Buddy Price, Jon Roberts, and Molly Turko. 2023. Redefining Recoverable Reserves in the Eagle Ford: Refracs and Infill Development Lessons Learned From the Hydraulic Fracturing Test Site 1 (HFTS) Phase 3. Paper SPE-212340-MS presented at the Hydraulic Fracturing Technology Conference and Exhibition, The Woodlands, TX.

Brady, Jared, Johan Daal, Kevan Marsh, Trevor Stokes, Pavan Vajjha, Rusty Werline, And Chris Williams. Impact of Re-Fracturing Techniques on Reserves: A Barnett Shale Example. Paper URTeC-2668825 presented at the Unconventional Resources Technology Conference, Austin, TX.

Bryan, Eric, Rex Richard, Connor Holasek, Nima Hosseinpour-Zonoozi, Dilhan Ilk, Charles Melvin, Kevin Eichinger, Brian Rankosky, Brian Ingalls, Sam French, Ken Day. 2023. Integrated Well Performance Analysis Methodology to Understand Production Performance and Identify Refracturing Candidates in Barnett Shale. Paper URTeC-3869654 presented at the Unconventional Resources Technology Conference, Denver, CO.

Cui, Alexander, Tim Gilberton, Dillon Niederhut. 2023. Revealing the Production Drivers for Refracs in the Willison Basin. Paper URTeC-3864951 presented at the Unconventional Resources Technology Conference, Denver, CO.

Dalkhaa, Chantsalmaa, Nicholas A. Azzolina, Alex Chakhmakhchev, Bethany A. Kurz, James A. Sorensen, Charles D. Gorecki, and John A. Harju. Refracturing in the Bakken – An Analysis of Data from Across

North Dakota. Paper URTeC-3723732 presented at the Unconventional Resources Technology Conference, Houston, TX.

Dontsov, Egor. 2022. A continuous fracture front tracking algorithm with multi layer tip elements (MuLTipEl) for a plane strain hydraulic fracture. Journal of Petroleum Science and Engineering **217**: 110841.

Eichinger, Kevin, Sam French, Ken Day, Jared Brady, Ryan Epperson, Richard
Leonard, and Brad Leonard. 2023. Hybrid Expandable Liner System: A Performance-Enhancing, Cost Effective Alternative to Bullhead Refracturing. Paper URTeC-3855094 presented at the Unconventional Resources Technology Conference, Denver, CO.

Fowler, Garrett, Jose Zaghloul, David Jones, Lindsey Hall-Wiist, Drew Hopson, Sarah Allen, Matteo Picone, Adrian Morales, Matteo Marongiu Porcu, Mark McClure, and Dave Ratcliff. 2023. A Success Story: Screening and Optimizing Refracs in the Eagle Ford. Paper URTeC-3848875 presented at the Unconventional Resources Technology Conference, Denver, CO.

Lindsay, G. J., D. J. White, G. A. Miller, J. D. Baihly, and B. Sinosic. 2016. Understanding the Applicability and Economic Viability of Refracturing Horizontal Wells in Unconventional Plays. Paper SPE-179113-MS presented at the Hydraulic Fracturing Technology Conference and Exhibition, The Woodlands, TX.

Mark McClure, Matteo Picone, Garrett Fowler, Dave Ratcliff, Charles Kang, Soma Medam, and Joe Frantz. 2020. Nuances and Frequently Asked Questions in Field-Scale Hydraulic Fracture Modeling. Paper SPE-199726-MS presented at the Hydraulic Fracturing Technology Conference and Exhibition, The Woodlands, TX.

McClure, Mark, Charles Kang, Chris Hewson, Soma Medam, Egor Dontsov, Ankush Singh, Carlo Peruzzo, and Elizaveta Gordeliy. 2024. ResFrac Technical Writeup. 18th Edition. arXiv:1804.02092.

Miller, Grant, Garrett Lindsay, Jason Baihly, and Tao Xu. 2016. Parent Well Refracturing: Economic Safety Nets in an Uneconomic Market. Paper SPE-180200-MS presented at the Low Perm Symposium, Denver, CO.

Morales, Adrian, Ke Zhang, Kush Gakhar, Matteo Marongiu Porcu, Don Lee, Dan Shan, Raj Malpani, Tim Pope, David Sobernheim, and Andrew Acock. 2016. Advanced Modeling of Interwell Fracturing Interference: An Eagle Ford Shale Oil Study – Refracturing. Paper SPE-179177-MS presented at the Hydraulic Fracturing Technology Conference and Exhibition, The Woodlands, TX.

Rezaei, Ali, Mehdi Rafiee, Statoil, Giorgio Bornia, Mohamed Soliman, and Stephen Morse. 2017. Protection Refrac: Analysis of Pore Pressure and Stress Change Due
to Refracturing of Legacy Wells. Paper URTeC-2667433 presented at the Unconventional Resources Technology Conference, Austin, TX.

Singh, Ankush, Mohsen Babazadeh, Craig Cipolla, Karan Dhuldhoya, Arjang Gandomkar, John Lassek, Ripu Manchanda, Michael McKimmy, Daniel Ramirez-Tamayo, Reza Safari, Mojtaba Shahri, Steve Smith, and Mark McClure. 2025. Far-field Drainage along Hydraulic Fractures: Insights from Integrated Modeling Studies in the Bakken and Permian Basin. Paper SPE-223567-MS presented at the Hydraulic Fracturing Technology Conference and Exhibition, The Woodlands, TX.

Velasquez, Cesar, and S. Hamed Tabatabaie. 2023. Screening and Ranking of Refractured Well Candidates: Insights from Performance Analysis of 14 Unconventional Plays Using Machine Learning Approach. Paper URTeC-3861457 presented at the Unconventional Resources Technology Conference, Denver, CO.